Annals of Biomedical Engineering, Vol. 23, 531–542, 1995
Printed in the USA.

0090-6964/95 $10.50 + .00

Wavelets in Biomedical Engineering

METIN AKAY

Department of Biomedical Engineering, Rutgers University

Abstract—Wavelets analysis methods have been widely used in the signal processing of biomedical signals. These methods represent the temporal characteristics of a signal by its spectral components in the frequency domain. In this way, important features of the signal can be extracted in order to understand or model the physiological system. This paper reviews the widely used orthogonal wavelet transform method in the biomedical applications.

Keywords—Biomedical signal analysis, Time-scale, Orthogonal wavelet transform.

INTRODUCTION

Fourier methods are widely used tools in signal processing (1,2). They relate the temporal characteristics of a signal with its frequency spectrum by writing the signal as an infinite summation of weighted sine and cosine waves of multiples of the fundamental frequency. However, an underlying assumption in these methods is the periodic nature of the signals (1,2). As a result, Fourier methods are not generally an appropriate approach in the analysis of signals with transient components (1).

Nonetheless, Fourier methods have been widely used in the analysis of biomedical signals that may have sharp transients. In order to identify any irregularity of the signal, it is common to divide long-term signals into blocks of short duration. This approach is known as the Short-Time Fourier Transform (STFT) method. The problem with STFT, however, is that a short analysis window smears the power of the signal and fails to represent the signal properly because of low spectral resolution. Accordingly, the spectral resolution of the STFT can be improved with the use of a longer data window. Unfortunately, this compromises the assumption of stationarity within the window.

Although the idea of analyzing signals at different scales or resolutions has existed since the beginning of the century (5,11–15,18–20,23,25,26,32,33), wavelet theory was tied together only recently through the work of Grossman and Morlet (14), who used the wavelet transform to model sound waves. Instead of using the Fourier transform, with its sine and cosine functions, they used finite length functions called wavelets. Wavelets were introduced as a signal representation in which an analysis window that is chosen to be short at high frequencies and long at low frequencies (to pick up all the abrupt changes) is used to analyze a signal. This method corresponds to having the frequency response logarithmically scaled along the frequency axis, as opposed to the short time Fourier transform, which uses a fixed window in the time domain.

The basis functions for wavelet transforms are wavelets (5,11–15). They need not have infinite duration and can be nonzero over a small period of the wavelet function. This compact support allows the wavelet transform to translate a time-duration function into a representation that is localized not only in frequency but in time as well. The time scale methods act as a "mathematical microscope" through which one can observe different parts of the signal by adjusting the focus. Figure 1 shows a wavelet decomposition of the electrocardiograph (ECG) signal. The ECG from a normal subject is shown in Fig. 1A. Fig. 1B shows the wavelet decomposition of the signal shown in Fig. 1A from the fine scales (high frequency bands) to the coarse scale (low frequency bands) in the time domain. Note that the representation has good time resolution at high frequencies and good frequency resolution at low frequencies (5,7–15). This exceptional ability of the wavelet transform has led to many new developments in fields of signal analysis, control, analysis of multifractal processes, image processing, and data compression.

In this paper, a brief introduction to wavelets is presented with a discussion of the design and implementation of the orthonormal wavelet transforms which have been widely used in the biomedical applications.

WAVELET TRANSFORM

The wavelet transform is a decomposition of the signal onto a set of basis functions. There are two basis functions in the design of a wavelet transform system. The first one is the scaling function, $\phi(t)$, which is called the basic dilation function. The second one is the primary wavelet

Address correspondence to M. Akay, Department of Biomedical Engineering, Rutgers University, P.O. Box 909, Piscataway, NJ 08855, U.S.A.

(Received 20May94, Revised 18Aug94, Revised 21Dec94, Accepted 7Jun95)

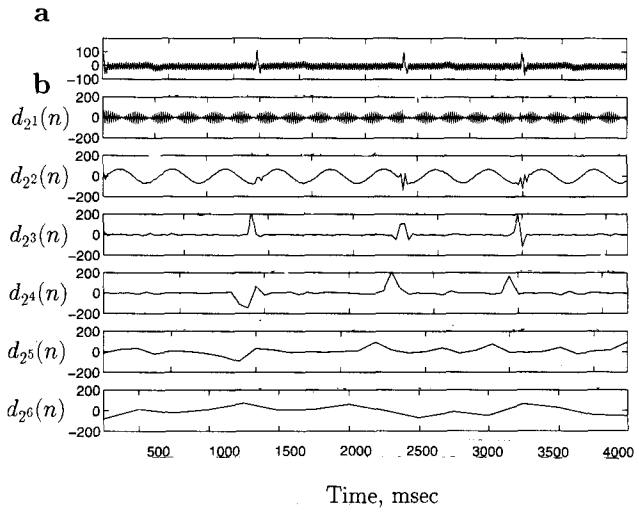

FIGURE 1. (a) Recording of a ECG signal from a normal subject. (b) Wavelet decomposition of the ECG signal shown in a.

function $\psi(t)$. Both of these are prototypes of a class of wavelet basis functions.

A wavelet function must satisfy two constraints (18,23). It must decay with respect to time, that is,

$$\lim_{t\to\infty} |\psi(t)| = 0, \tag{1}$$

where the rate of decay depends upon the function chosen. Secondly, its integral over all time must vanish.

$$\int_{-\infty}^{\infty} \psi(t)dt = 0. \tag{2}$$

These two conditions guarantee that the wavelet function is well localized and that it oscillates like a wave.

The integral of the scaling function is not equal to zero and can be assumed to be

$$\int_{-\infty}^{\infty} \phi(t)dt = 1. \tag{3}$$

The relationship between the scaling and wavelet functions is given as follows:

$$\phi(t) = \phi(2t) + \phi(2t - 1), \tag{4}$$

$$\psi(t) = \phi(2t) - \phi(2t - 1). \tag{5}$$

Given a continuous input signal $x(t)$, the continuous wavelet transform (CWT) can be defined as

$$X_{CWT}(a, b) = \int x(\gamma)\psi^*_{a,b}(\gamma)d\gamma \tag{6}$$

where * denotes complex conjugation,

a represents the scaling factor,

b represents the time

$\psi_{a,b}(t)$ is obtained by scaling the prototype wavelet ψ(t) at time b and scale a so that

$$\psi_{a,b}(t) = \frac{1}{\sqrt{|a|}}\psi\left(\frac{t-b}{a}\right) \tag{7}$$

for $a, b \in R^+$. Note that R^+ represents the real numbers.

It is noteworthy that, in the Eq. 7, when a becomes large, the basis function $\psi_{a,b}$ becomes a stretched version of the prototype. This can be useful for the analysis of the low-frequency components of the signal. On the other hand, when the scale factor is small, the basis function $\psi_{a,b}$ will be contracted. This is useful for the analysis of the high frequency components of the signal.

The factor $\frac{1}{\sqrt{|a|}}$ in Eq. 7 was introduced to guarantee energy preservation (23).

The discrete wavelet transform (DWT) can be obtained by discretizing the parameters a and b. One possible way to do so is to sample the time-scale parameters on a "dyadic" grid (basis 2) in the time-scale plane (18) for the wavelet and scaling parameters. Then,

$$\psi_{j,k}(n) = 2^{\frac{-j}{2}}\psi(2^{-j}n - k), \tag{8}$$

$$\phi_{j,k}(n) = 2^{\frac{-j}{2}}\phi(2^{-j}n - k), \tag{9}$$

where $j \in Z$, $k \in Z$, $a = 2^j$, $b = k2^j$ and 2^{-j} represents the resolution. Note that the parameter Z represents the set of integers. All the integral limits can be assumed to be from $-\infty$ to ∞ unless stated. The basis 2 was chosen to simplify the computations (14). Note that the discrete parameter j controls the dilation or compression of the scaling and wavelet functions. On the other hand, the parameter k controls the translation in time.

Orthogonal Wavelet Transform

The orthogonal spline wavelet transform was proposed by Battle and Lemarie (5) and implemented by Mallat (18) to analyze the contents of images and signals. Later, Daubechies (11–13) constructed the compactly supported orthogonal wavelet transform.

For the orthonormal case, the wavelet and scaling functions can be estimated as follows:

$$\psi(n) = \sum_k h(k)\phi(2n - k) \tag{10}$$

and

$$\phi(n) = \sum_k g(k)\phi(2n - k) \tag{11}$$

where the $h(n)$ and $g(n)$ are called the wavelet and scaling filter coefficients.

A discrete signal $x(n)$, $n \in Z$, can be expanded onto the scaling function $\phi(n)$ at level $j = 0$ as follows:

$$x(n) = \sum_k a_k \phi(n - k) \tag{12}$$

This data sequence can be further decomposed into its components along D_{2^j} A_{2^j} for the level $j = 1$ as follows:

$$x(n) = D_{2^1}[x(n)] + A_{2^1}[x(n)] \tag{13}$$

Where $A_{2^1}[x(n)]$ represents the approximate signal at level $j = 1$, and $D_{2^1}[x(n)]$ is the detail signal at level $j = 1$ representing the difference in information between the versions of $x(n)$ at two successive resolution levels (here, between the original signal and the approximate signal at level $j = 1$).

The approximate signal $A_{2^1}[x(n)]$ and detail signal $D_{2^1}[x(n)]$ at level $j = 1$ can be further written as,

$$D_{2^1}[x(\mathrm{n})] = \sum_{k \in Z} d_{2^1}(k) \psi_2(n - 2k) \tag{14}$$

$$A_{2^1}[x(n)] = \sum_{k \in Z} a_{2^1}(k) \phi_2(n - 2k) \tag{15}$$

where $\psi_{2^1}(n - 2^1 k)$ are the analysis wavelets and $\phi_{2^1}(n - 2^1 k)$ are the scaling sequences. These are the discrete versions of the continuous wavelet $\psi_{2^1}(t - 2^1 k)$ and the scaling function $\phi_{2^1}(t - 2^1 k)$; $d_{2^1}(k)$ are the wavelet coefficients, or the detailed signals at scale 2^1; $a_{2^1}(k)$ are the scaling coefficients, or the approximated signal at scale 2^1.

Given a discrete signal $x(n)$, $n \in Z$, its discrete wavelet transform (DWT) up to a level J of depth (its multiresolution decomposition on J octaves) is defined as

$$x(n) = \sum_{j=1}^{J} \sum_{k \in Z} d_j(k) \psi^r_{2^j}(n - 2^j k) + \sum_{k \in Z} a_J(k) \phi_{2^J}(n - 2^J k) \tag{16}$$

where $\psi^r_{2^j}(n - 2^j k)$ are the analysis wavelets and $\phi_{2^J}(n - 2^J k)$ are the scaling sequences. These are the discrete versions of the continuous wavelet $\psi^r_{2^j}(n - 2^j k)$ and the scaling function $\phi_{2^J}(n - 2^J k)$; $d_{2^j}(k)$ are the wavelet coefficients, or the detailed signals at scale 2^j; $a_{2^J}(k)$ are the scaling coefficients, or the approximated signal at scale 2^J.

Note that the wavelet coefficients $d_{2^j}(n)$ represent the details of the original signal at different levels of resolution. The scaling coefficients a_{2^j} represent the approximation of the original signal $x(n)$ with a resolution of one point for every 2^j points of the original signal.

The sequence a^{2_1} at level $j = 1$ represents the approximated (smoothed) version of the original data sequence $x(n) = a_{2^0}(\mathrm{n})$. However, the $d_{2^1}(n)$ represents the difference in information between $a_{2^0}(n)$ and $a_{2^1}(n)$.

The data sequences $a_{2^1}(n)$ and $d_{2^1}(n)$ at level $j = 1$ can be computed as a function of $a_{2^0}(n)$ at level $j = 0$ as follows:

$$a_{2^1}(n) = \phi_{2^1}(n) * x(n) \sum_k x(k) < \phi_{2^1}(n), \phi(k) > \tag{17}$$

Note that the operator $< \phi_{2^1}(m), \phi(k) >$ represents the inner product of the functions $\phi_{2^1}(k)$ and $\phi(m)$, and can be further written as

$$< \phi_2(m), \phi(k) \geqslant 2^{-1/2} \int_t \phi(t - m) \phi(t - k) dt \tag{18}$$

Eq. 17 can be further written as follows:

$$a_{2^1}(n) = \sum_k g(k - 2^1 n) a_{2^0}(k) \tag{19}$$

where $g(n) = 2^{-1/2} \int_t \phi\left(\frac{1}{2}\right) \phi(t - n) dt.$

Similarly, the detail signal can be estimated as follows:

$$d_{2^1}(n) = \sum_k h(k - 2^1 n) a(k) \tag{20}$$

where $h(n) = 2^{-1/2} \int_t \psi\left(\frac{1}{2} t\right) \phi(t - n) dt.$

Note that the scaling filter coefficients $h(n)$ can be assumed to be a difference operator (highpass filter) and the wavelet filter coefficients $g(n)$ as an averaging operator (lowpass filter). The detail and approximate signals can be estimated in terms of the filter coefficients $h(n)$ associated with the wavelet function and the coefficients $g(n)$ associated with the scaling function. The detailed signals $d_{2^1}(n)$ at level $j = 1$ are calculated by convolving the signal $x(n) = a_{2^0}(n)$ at level $j = 0$ with the filter coefficients $h(n)$ associated with the wavelet function as follows (1,13)

$$d_{2^1}(n) = \sum_k h(k - 2^1 n) a(k) = h(n) * a_0(n) \tag{21}$$

and the scaling coefficients $a_{2^1}(n)$ can be computed by convolving the signal $x(n) = a_{2^0}(n)$ at level $j = 0$ with the filter coefficients $g(n)$ associated with the scaling function $\phi_{2^j}(n)$ as follows

$$a_{2^1}(n) = \sum_k g(k - 2^1 n) a(k) = g(n) * a(n) \tag{22}$$

The procedure can be iterated at scale $j = 2$ as follows:

$$A_{2^1}[x(n)] = D_{2^2}[x(n)] + A_{2^2}[x(n)] \tag{23}$$

where $D_{2^2}[x(n)] = \Sigma_{k\in Z} d_{2^2}(k)\psi_{2^2}(n - 2^2k)$ and $A_{2^2}[x(n)] = \Sigma_{k\in Z} a_{2^2}(k)\phi_{2^2}(n - 2^2k)$. Note that the detail signal $d_{2^2}(n)$ can be estimated in terms of the filter coefficients as follows:

$$d_{2^2}(n) = \sum_k h(k - 2n)a_{2^1}(k) = h(n) * a_{2^1}(n) \tag{24}$$

Similarly, the approximate signal $a_{2^2}(n)$ can be estimated as follows:

$$a_{2^2}(n) = \sum_k g(k - 2n)a_{2^1}(k) = g(n) * a_{2^1}(n) \tag{25}$$

As a summary, this procedure can be iterated until $j = \log_2 N$ where N is the length of the data sequence $x(n)$:

$$\begin{aligned} A_{2^{j-1}}[x(n)] &= A_{2^j}[x(n)] + D_{2^j}[x(n)] \\ &= \sum_{k\in Z} d_{2^j}(k)\psi_{2^j}(n - 2^jk) \\ &\quad + \sum_{k\in Z} a_{2^j}(k)\phi_{2^j}(n - 2^jk) \end{aligned} \tag{26}$$

using $a_{2^j}(n) = g(n) * a_{2^{j-1}}(n)$ and $d_{2^j}(n) = h(n) * a_{2^{j-1}}(n)$

Note that the successive a_{2^j} are lower and lower resolution version of the orginal data sequence $x(n) = a_{2^0}(n)$, each sampled twice as sparsely as their predecessor due to the factor 2 in the filter functions $g(n)$ and $h(n)$.

Thus, the decomposition and reconstruction of the detail and approximate signals can be computed using a tree algorithm as described below.

As a summary, the wavelet transform determines the values of detail and approximate signals at each scale. The estimation of the signals at scale j can be done by simply convolving the approximate signal at scale $j - 1$ with the wavelet filter coefficients $h(n)$ to estimate the detail signal at scale j, and with the scaling filter coefficients $g(n)$ to estimate the approximate signal at scale j. Therefore, in order to implement the wavelet transform, we should estimate the appropriate wavelet and scaling filters $h(n)$ and $g(n)$.

Design of Orthogonal Wavelet Transform

The design of a wavelet system involves the estimate of the scaling function $\phi(t)$, and the wavelet and scaling filters $h(n)$ and $g(n)$. The wavelet system can be designed either by choosing the scaling function $\phi(t)$, or by choosing the appropriate scaling and wavelet filters $g(n)$ and $h(n)$.

In practice, the wavelet design can be started first by choosing the scaling function using either the linear spline function or the quadratic spline function. These bases are known as the Battle-Lemarie bases.

Using the linear spline function, we can obtain the scaling function $\phi(t)$ as follows:

$$\phi(t) = \begin{bmatrix} t & 0 \leq t \leq 1 \\ 2 - t & 1 \leq t \leq 2 \\ 0 & otherwise \end{bmatrix} \tag{27}$$

Then, the scaling function obtained from the linear spline function can be written as follows:

$$\phi(t) = \frac{1}{2}\phi(2t) + \phi(2t - 1) + \frac{1}{2}\phi(2t - 2) \tag{28}$$

Therefore, the coefficients of the scaling filter $g(n)$ can be taken as the weights of the right hand side of the Eq. 28 as described in Eq. 11.

Using the quadratic spline function, we can obtain the scaling function $\phi(t)$ as follows:

$$\phi(t) = \begin{bmatrix} t^2 & 0 \leq t \leq 1 \\ -2t^2 + 6t - 3 & 1 \leq t \leq 2 \\ (3 - t)^2 & 2 \leq t \leq 3 \\ 0 & otherwise \end{bmatrix} \tag{29}$$

Then, the scaling function obtained from the quadractic spline function can be written as follows:

$$\begin{aligned} \phi(t) &= \frac{1}{4}\phi(2t) + \frac{3}{4}\phi(2t - 1) + \frac{3}{4}\phi(2t - 2) \\ &\quad + \frac{1}{4}\phi(2t - 3) \end{aligned} \tag{30}$$

Note that the wavelet filter coefficients of the $h(n)$ can be taken as the weights the right hand side of the Eq. 30. After estimating the wavelet filter coefficients $h(n)$, the wavelet function $\psi(t)$ can be estimated using Eq. 5.

Although the construction of the Battle-Lemarie bases are easily obtained, the resulting scaling function for each scale may not be compactly supported and may cause the wavelet function $\psi(t)$ to become non-compactly supported wavelet functions $\psi(t)$ for each scale j. In order to overcome this difficulty, Mallat (18) and Daubechies (11–13) designed a wavelet system from the scaling filter $g(n)$ and wavelet filter $h(n)$ instead of the scaling function $\phi(t)$. The coefficients $h(n)$ and $g(n)$ are associated with the wavelet and scaling functions, respectively. The filters $h(n)$ and $g(n)$ associated with the wavelet and scaling functions have the following properties:

1. $\Sigma_k |g(k)| < \infty$
2. $\Sigma_k |h(k)| < \infty$
3. $\Sigma_k g(2k + 1) = \Sigma_k g(2k)$.

4. $\Sigma_k\, g(k) = \sqrt{(2)}$ since $\int \phi(t)dt \neq 0$
5. $\Sigma_k\, h(k) = 0$ since $\int \psi(t)dt = 0$
6. $\Sigma_k\, g(k - 2m)g(k - 2l) = \delta_{ml}$
7. $\Sigma_k\, h(k - 2m)h(k - 2l) = \delta_{ml}$
8. $\Sigma_k\, g(k - 2m)g(k - 2l) + \Sigma_k\, h(k - 2m)h(k - 2l) = \delta_{ml}$
9. $\Sigma_n\, g(n - 2k)h(n - 2l) = 0$ since $< \phi_{2j,k}, \psi_{2i,m} \geq 0$

As described elsewhere (18), using the properties given above, the scaling filter coefficient $g(n)$ can be estimated, the wavelet filter coefficients $h(n)$ can be from $h(n) = (-1)^n\, g(3 - n)$.

As described above, if the impulse response filter $g(n)$ has finite nonzero length, $g(n) = 0$ for $n < N_-$ or $n > N_+$ and the wavelet filter function $h(n) = 0$ for $n < -N_+ + 1$ or $n > -N_- + 1$. Then, the corresponding scaling and wavelet functions will have compact support. The main emphasis of this approach was on the derivation of the impulse filters $h(n)$ and $g(n)$. These impulse functions are such that $h(n)$ is an even function and $g(n)$ is symmetric around the axis ½. Both of these functions are regular and may not have compact support.

TABLE 1. $g_N(n)(n = 0, 1, 2, 3, \ldots, 2N - 1)$ for $N = 2, 3, 4, 5, 6$.

N	n	$g_N(n)$
$N = 2$	0	.482962913145
	1	.836516303738
	2	.224143868042
	3	−.129409522551
$N = 3$	0	.332670552950
	1	.806891509311
	2	.459877502118
	3	−.135011020010
	4	−.085441273882
	5	.035226291882
$N = 4$	0	.230377813309
	1	.714846570553
	2	.630880767930
	3	−.027983769417
	4	−.187034811719
	5	.030841381836
	6	.032883011667
	7	−.010597401785
$N = 5$	0	.160102397974
	1	.603829269797
	2	.724308528438
	3	.138428145901
	4	−.242294887066
	5	−.032244869585
	6	.077571493840
	7	−.006241490213
	8	−.012580751999
	9	.003335725285
$N = 6$	0	.111540743350
	1	.494623890398
	2	.751133908021
	3	.315250351709
	4	−.226264693965
	5	−.129766867567
	6	.097501605587
	7	.027522865530
	8	−.031582039318
	9	.000553842201
	10	.004777257511

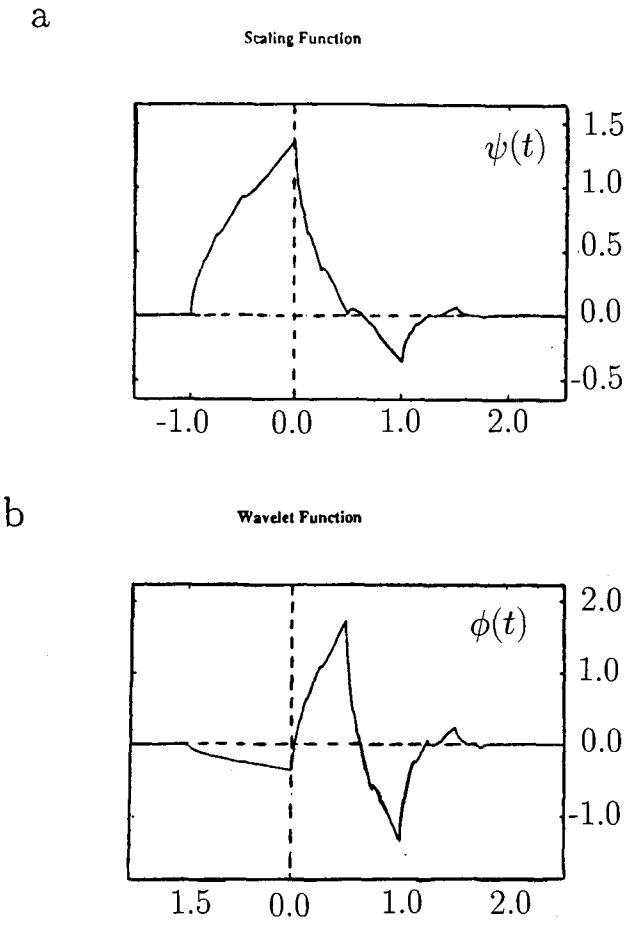

FIGURE 2. (a) Scaling function. (b) Wavelet function of the compactly supported wavelet transform method.

Daubechies (11–13) constructed orthonormal bases of compactly supported wavelets by estimating the finite length impulse function $g(n)$ satisfying the following conditions:

1. $\Sigma_k\, |g(k)||k|^\epsilon < \infty$
2. $\Sigma_k\, g(k - 2m)g(k - 2l) = \delta_{ml}$
3. $\Sigma_g\, (k) = \sqrt{(2)}$ for $\Sigma_n\, |x(n)||n|^\epsilon < \infty$

where $\epsilon > 0$.

The scaling filter g(n) which satisfies all the necessary conditions for $n = 0, 1, 2, 3$ was described by Daubechies as follows:

1. $g(0) = 2^{-0.5}\, \mu \dfrac{(\mu - 1)}{(\mu^2 + 1)}$

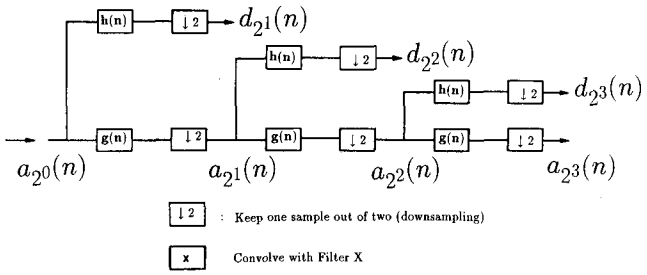

FIGURE 3. Implementation of orthogonal wavelet decomposition algorithm using a tree structure.

$$2.\ g(1) = 2^{-0.5}\frac{(1-\mu)}{(\mu^2+1)}$$

$$3.\ g(2) = 2^{-0.5}\frac{(\mu-1)}{(\mu^2+1)}$$

$$4.\ g(3) = 2^{-0.5}\,\mu\frac{(\mu-1)}{(\mu^2+1)}$$

The wavelet filter $h(n)$ can be estimated as $h(n) = (-1)^n g(3-n)$ as,

$$1.\ h(0) = 2^{-0.5}\,\mu\frac{(\mu-1)}{(\mu^2+1)}$$

$$2.\ h(1) = -2^{-0.5}\frac{(\mu-1)}{(\mu^2+1)}$$

$$3.\ h(2) = 2^{-0.5}\frac{(\mu-1)}{(\mu^2+1)}$$

$$4.\ h(3) = -2^{-0.5}\,\mu\frac{(\mu-1)}{(\mu^2+1)}$$

All the other values of $h(n)$ and $g(n)$ are equal to zero.

Figure 2 shows the scaling factor $\phi(t)$ and the wavelet function $\psi(t)$ for $\mu = -\frac{1}{\sqrt{3}}$ with support width $N_+ - N_- = 3(N_+ = 3, N_- = 0)$. Note that the scaling and wavelet functions are not symmetric functions unlike the Battle-Lemaire wavelets discussed above. The details and mathematical derivations of the compactly supported orthonormal wavelet transform are described elsewhere (11–13). Table 1 summarizes the filter coefficients of the impulse function g(n) ($n = 0, \ldots, 2N-1$) for $N = 2, 3, 4$, and 5.

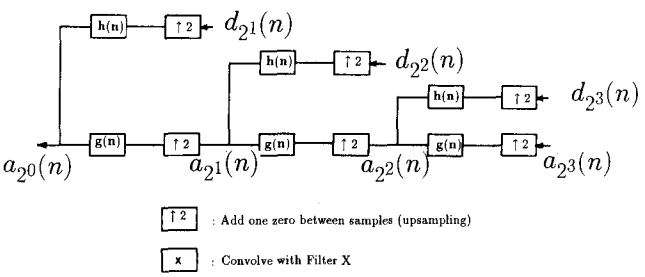

FIGURE 4. Implementation of orthogonal wavelet reconstruction algorithm using a tree structure.

Implementation of Orthogonal Wavelet Transforms

Mallat (18) and Daubechies (13) recently showed that the wavelet transform can be implemented with a specially designed pair of finite impulse response (FIR) filters. The FIR filters are known as quadrature mirror filters (QMF) in which the frequency responses of the two FIR filters separate the high-frequency and low-frequency component of the input signal. The output of the QMF filter pair are decimated (or desampled) by a factor of two; that is, every other output sample of the filter is kept and the others are discarded. The low-pass filter output is fed into another identical QMF filter pair. This process can be repeated recursively as a tree or pyramid algorithm.

Mallat (18) showed that the tree or pyramid algorithm can be applied to the wavelet transform by using the low-pass and high-pass filters. The high filter is associated with the $h(n)$ coefficients of the wavelet function $\psi(n)$ and the low-pass filter is associated with the $g(n)$ coefficients of the scaling function $\phi(n)$. The impulse filter responses $h(n)$ and $g(n)$ are the filter coefficients of the QMF filter pairs. Note that the output of each low-pass filter is the $d_{2^j}(n)$ or detailed signal of the original signal at resolution 2^{2^j}. The output of each high-pass filter is the $a_{2^j}(n)$ or approximated signal at resolution 2^j. The approximate signal $a_{2^j}(n)$ of the previous level can be used to generate the new $a_{2^j}(n)$ and $d_{2^j}(n)$ for the next level of tree. It is noteworthy to mention that the original signal $x(n)$ has N samples. However, the approximated and the detailed signals will only have 2^jN samples each, for $J \geq j \geq 1$ because of the downsampling process. Note that J represents the number of maximum wavelet scales.

As a summary, the orthogonal spline wavelet representation can be computed by successively decomposing $a_{2^{j-1}}(n)$ into $a_{2^j}(n)$ and $d_{2^j}(n)$ for $J \geq j \geq 1$. The procedure can be outlined as follows (1, 13, 18):

Initially the impulse response coefficients of the digital filters $h(n)$ and $g(n)$ that are associated with the wavelet and scaling functions should be determined.

Step 1: At scale $j = 0$, the approximated signal $a_{2^0}(n)$ can be given as $a_{2^0}(n) = x(n)$.

Step 2: Calculate the approximated signal at each scale 2^j by convolving the approximated signal $a_{2^{j-1}}(n)$ with the digital filter $g(n)$ and keep every other sample of the outcome of the convolution process (downsampling) as follows $a_{2^j}(n) = [g * a_{2^{j-1}}(n)] \downarrow_2$

Step 3: Calculate the detailed signal at each scale 2^j by convolving the approximate signal $a_{2^{j-1}}(n)$ with the digital filter $h(n)$ and keep every other sample

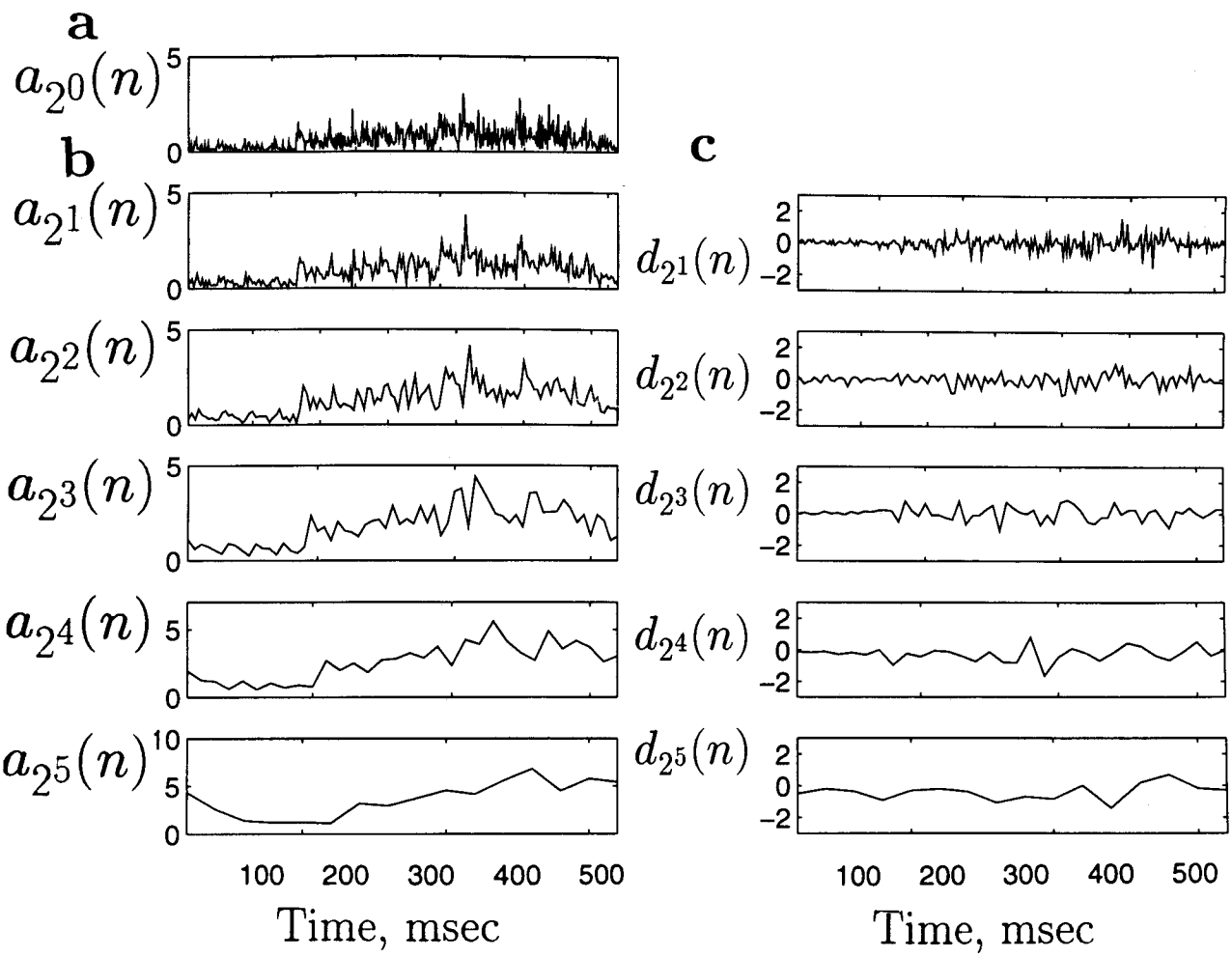

FIGURE 5. (a) Recording of a phrenic neurogram activity from a cat. (b) Approximate signals, $a_{2^j}(n)$ using the orthogonal wavelet transform. (c) Detail signals, $d_{2^j}(n)$ using the orthogonal wavelet transform.

of the outcome of the convolution process (downsampling) as follows $d_{2^j}(n) = [h * a_{2^{j-1}}(n)] \downarrow_2$

Step 4: If $j \leq J$ go to the next iteration ($j = j + 1$).

The block diagram of the wavelet decomposition algorithm is shown in Fig. 3.

The reverse wavelet transform essentially performs the operations in the reverse direction. The process works down the branches of the tree combining the approximation and detail signals into approximate signal with higher levels of detail. Note that in the reconstruction process, instead of decimation, the signals are interpolated by putting zeros between each value of the approximate and detail signals, and these signals are then filtered using the high-pass and low-pass filters. The intermediate zero values are then replaced by estimates derived from the convolutions. The filter outputs at that level are later summed to create the approximate signal for the next higher level of resolution. The final set of approximation signals at the tree's top level in the reverse transform is a reconstruction of the original signal.

The original signal can be reconstructed by putting zeros between each sample of $a_{2^j}(n)$ and $d_{2^j}(n)$ (upsampling) and convolving the resulting signal with the filters $h(n)$ and $g(n)$. The reconstruction algorithm can be implemented as follows:

$$a_{2^{j-1}}(n) = \sum_m a_{2^j}(m) < \phi_{2^{j-1}}(m), \phi_{2^j}(n) > + \sum_m d_{2^j}(m) < \phi_{2^{j-1}}(m), \psi_{2^j}(n) > \quad (31)$$

or

$$a_{2^{j-1}}(n) = \sum_k g(n - 2k)a_{2^j}(k) + \sum_k h(n - 2k)d_{2^j}(k) = g(n) * a_{2^j} + h(n) * d_{2^j} \quad (32)$$

for $J \geq j \geq 1$.

As a summary, the orthogonal spline wavelet reconstruction at level $j - 1$ $a_{2^{j-1}}(n)$ can be computed by suc-

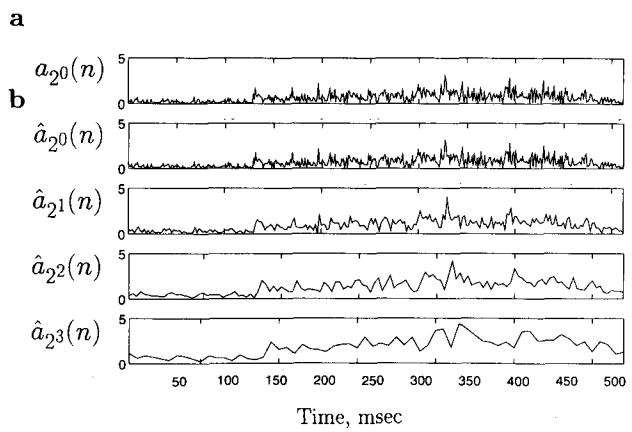

FIGURE 6. (a) Recording of phrenic neurogram activity from a cat shown in Fig. 5a. (b) Reconstruction of the signal shown in Fig. 6a using the orthogonal wavelet transform at different levels.

cessively combining $a_{2^j}(n)$ and $d_{2^j}(n)$ for $J \geq j \geq 1$. The procedure is outlined as follows, assuming that the impulse response of the digital filters $h(n)$ and $g(n)$ associated with the wavelet and scaling functions at scale $j = J$ are known; the approximate signal and detail signals at $j = J$ are also known:

Step 1: Upsample the approximate signal at level j before convolving with the filter function $g(n)$ by putting zeros between their samples (upsampling).

$$a_{2^{j-1}}(n) = [g * [a_{2^j}(n)] \uparrow_2]$$

Step 2: Upsample the detail signal at level j before convolving with the filter function $h(n)$ by putting zeros between their samples (upsampling).

$$d_{2^{j-1}}(n) = [g * [d_{2^j}(n)] \uparrow_2]$$

Step 3: Calculate the approximated signal $a_{2^{j-1}}(n)$ at each scale $j - 1$, by combining the outcomes of step 1 and step 2

Step 4: If $j \geq 1$ go to the next iteration ($j = j - 1$).

The block diagram of the wavelet reconstruction algorithm is shown in Fig. 4.

It is suggested that the readers refer to References 11–13 for the details of the compactly supported orthonormal wavelet transform. Note that as far as the implementation is concerned, the only difference between the Battle-Lemarie (18) and the compactly supported wavelet transform (11–13) is the form of impulse responses $h(n)$ and $g(n)$.

The orthogonal wavelet transform is computationally as efficient as the Fourier transform methods which require $N\log_2 N$ operations for a length of N data samples. Note that the orthogonal wavelet transform only requires N operations since in the tree structure at each scale j, only half the operations of its predecessor must be done.

The wavelet transforms have been used for detection of heart diseases (3), monitoring fetus maturation (4), magnetic resonance imaging (16), analysis of evoked responses (6, 30), pitch detection of speech signals (17), detection of late potentials (22), analysis of ECG of postinfarction patients (24), sound analysis (21), and auditory detection of acoustic signals (34). Reviews of wavelet theory applied to signal processing can be found in (1,25,26,28). A discussion about the optimal choice for the wavelet function is in (29). Readers are referred to references (1,7–10,15,19,20,27,28,31–33) regarding other types of wavelet transforms, including the wavelet packets, B-spline, and matching pursuits methods.

WAVELET ANALYSIS OF BIOLOGICAL SIGNALS

Here, we would like to discuss some potential applications of the wavelet transform to biological signals.

Analysis of Phrenic Neurogram

The objective of the analysis was to characterize eupnea (normal breathing) and to understand how system perturbations such as hypoxia result in alterations in respiratory patterning in both the time and frequency domains.

The phrenic neurogram activity recorded from a cat is shown in panel A of Fig. 5. In this figure, panel B and C show the wavelet transform [the wavelet approximation, $a_{2^j}(n)$ and the detail signal $d_{2^j}(n)$] of the phrenic neurogram signal of Fig. 5A, using the compactly supported orthogonal wavelet transform for $J \geq j \geq 1$.

Note that the phrenic activity has very complex characteristics in both the time and frequency domains. The detail signals in the first and second wavelet bands are prominent. The detail signals in the third and fourth wavelet bands increased after 250 msec of the whole breaths.

Fig. 6A again shows the original signal, and 6B shows the reconstructed signals at different levels for $j = 1, 2, 3, 4$. Note that the original signal shown in Fig. 6A was almost the same as the reconstructed signal shown in Fig. 6B at level $j = 1$.

Analysis of Diastolic Heart Sounds

The objective of the analysis was to investigate the use of wavelet analysis to analyze the turbulent sounds associated with coronary artery disease and to provide a simple, noninvasive approach for the detection of coronary artery disease.

The diastolic heart sounds recorded from a normal subject is shown in panel A of Fig. 7. In this figure, panels B and C show the wavelet approximation, $a_{2^j}(n)$, and the detail signal, $d_{2^j}(n)$, of the diastolic heart sound signal of Fig. 7A, using the compactly supported orthogonal wavelet transform for $5 \geq j \geq 1$.

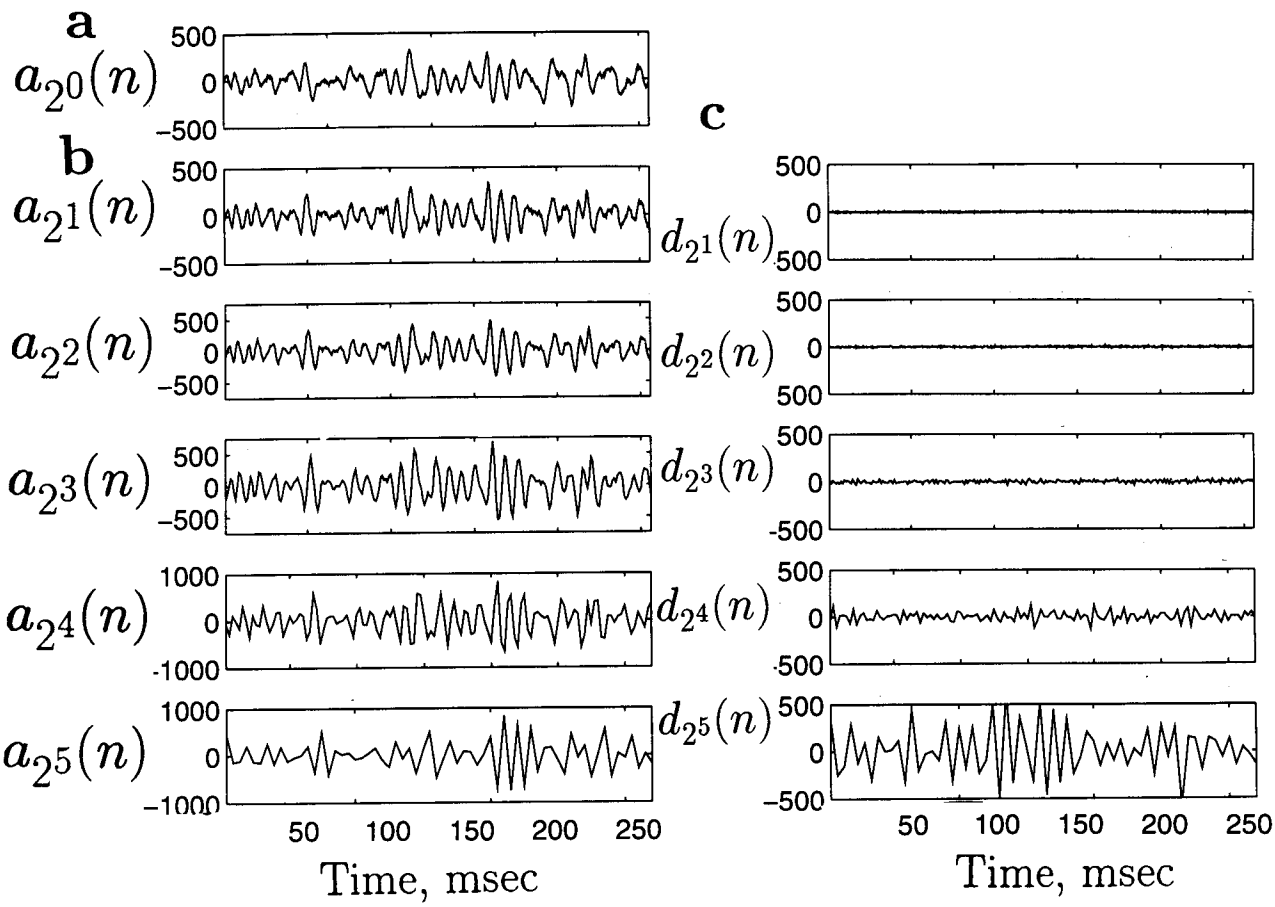

FIGURE 7. (a) Recording of a diastolic heart sound signal from a normal subject. (b) Approximate signals, $a_{2j}(n)$, using the orthogonal wavelet transform. (c) Detail signals, $d_{2j}(n)$ using the orthogonal wavelet transform.

Note that the detail signals from the normal subject have no activity in the first three wavelet bands. However, the detail signals in the fourth and especially the fifth wavelet bands are prominent, suggesting that the diastolic heart sounds from normal subjects do not have any significant high frequency components.

Fig. 8A again shows the original signal, and 8B shows the reconstructed signals at different levels for $j = 1, 2, 3, 4$. Note that the original signal shown in Fig. 8a was almost the same as the reconstructed signal shown in Fig. 8B at level $j = 1$.

Analysis of Evoked Response Activity

The objective of the analysis was to characterize the short latency evoked potentials that can be observed in human subjects following stimulation of respiratory mechanoreceptors. These respiratory-related evoked responses indicate the nature of afferent information entering the central regulatory and perception processes. We have recently explored the wavelet transform method for improved signal detection in noisy backgrounds, and applied the wavelet transform method to our data to determine whether we could obtain the essential characteristics of the signal in fewer trials than were previously required.

A five trial ensemble average of respiratory related

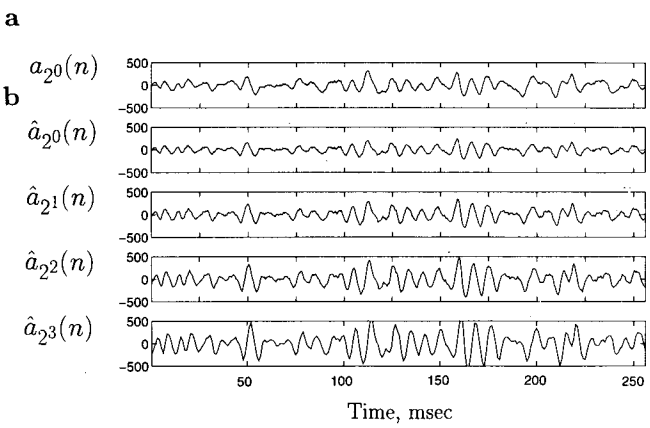

FIGURE 8. (a) Recording of a diastolic heart sounds signal from a normal subject. (b) Reconstruction of the signal shown in Fig. 7a. using the orthogonal wavelet transform at different levels.

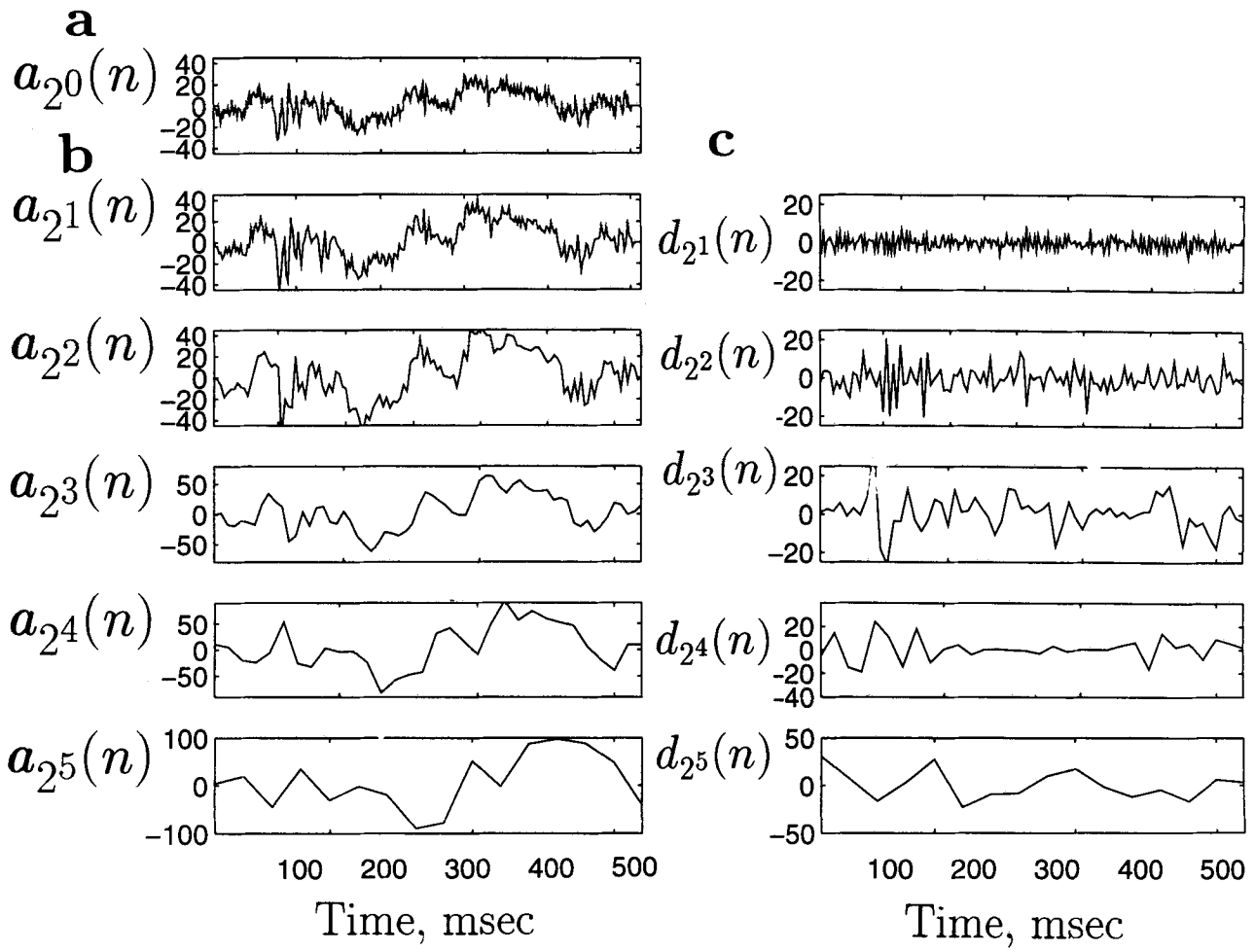

FIGURE 9. (a) Recording of a five trial ensemble average of respiratory related evoked responses from a normal subject. (b) Approximate signals, $a_{2^j}(n)$, using the orthogonal wavelet transform. (c) Detail signals, $d_{2^j}(n)$ using the orthogonal wavelet transform.

evoked responses from a normal subject, is shown in panel A of Fig. 9. In this figure, panels B and C show the wavelet approximation $a_{2^j}(n)$ and the detail signal $d_{2^j}(n)$ of the respiratory evoked response in Fig. 9A, using the compactly supported orthogonal wavelet transform for $5 \geq j \geq 1$.

Note that the respiratory evoked response signal used in this study has low frequency signal components throughout time, but intermediate frequency signal components only between 50–100 msec with several transients in time. The wavelet transform was able to localize the transients and the intermediate frequency components between 50–100 msec.

Fig. 10A again shows the original signal, and 10B shows the reconstructed signals at different levels for $j = 1, 2, 3, 4$. Note that the original signal shown in Fig. 10A was almost the same as the reconstructed signal shown in Fig. 10B at level $j = 1$.

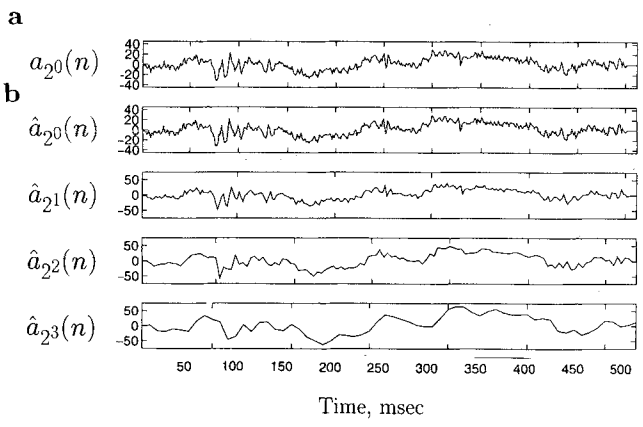

FIGURE 10. (a) Recording of a five trial ensemble average of respiratory related evoked responses from a normal subject shown in Fig 9a. (b) Reconstruction of the signal shown in Fig. 10a.

The readers are referred to (1) for details of all these applications.

CONCLUSION

In this paper, an introductory view of wavelet theory was developed for the reader unfamiliar with the field. The conditions for defining a wavelet, the processes of synthesis and analysis, and the computational implementation of widely-used wavelet transform methods were discussed. Applications of the wavelet transform methods to biomedical engineering were cited. In addition, applications of the compactly supported orthogonal wavelet transform to some biological signals were briefly presented.

Wavelet transform methods can be easily and quickly computed. Because the basis functions are finite, wavelets can provide accurate representation of fairly short signals, and they are useful for characterizing nonstationary signals and quantifying the differences in the signal between different states.

REFERENCES

1. Akay, M. Detection and Estimation of Biomedical Signals. San Diego: Academic Press, 1995.
2. Akay, M. *Biomedical Signal Processing*. San Diego: Academic Press, 1994.
3. Akay, M., G. Landesberg, W. Welkowitz, and D. Sapoznikov. Time-frequency analysis of heart rate fluctuations during carotid surgery using wavelet transform. In: *Comparative Approaches in Medical Reasoning,* edited by M. Cohen and D. Hudson. New York: World Scientific Publishing Co., 1995 (in press).
4. Akay, M., P. Chung, and H. H. Szeto. Time-frequency analysis of the electrocortical activity during maturation using wavelet transform. *Biol. Cybernetics* 71:169–176, 1994.
5. Battle, G. A block spin construction of ondelettes, part I: Lemarie functions. *Comm. Math. Phys.* 110:601–615, 1987.
6. Bertrand, O., J. Bohorquez, and J. Pernier. Time-frequency digital filtering based on an invertible wavelet transform: An application to evoked potentials. *IEEE Trans. Biom. Eng.* 41:77–87, 1994.
7. Chui, C. K. *An Introduction to Wavelets*. San Diego: Academic Press, 1992.
8. Coifman, R., and G. Weiss. Extensions of Hardy spaces and their use in analysis. *Bull. Amer. Math. Soc.* 83:569–645, 1977.
9. Coifman, R., Y. Meyer, S. Quake, and V. Wickerhauser. *Signal Processing and Compression with Wavelet Packets*. Numerical Algorithms Research Group Report, Yale University, 1990.
10. Coifman, R. and V. Wickerhauser. Entropy-based algorithms for best basis selection. *IEEE Trans. Info. Theory* 38:713–718, 1992.
11. Daubechies, I. Time-frequency localization operators: A geometric phase space approach. *IEEE Trans. Info. Theory* 34:605–612, 1988.
12. Daubechies, I. Orthonormal bases of compactly supported wavelets. *Commun. Pure Applied Math.* 41:909–996, 1988.
13. Daubechies, I. *Ten Lectures on Wavelets*. Society for Industrial and Applied Mathematics, 1992.
14. Grossman, A., and J. Morlet. Decomposition of Hardy functions into square integrable wavelets of a constant shape. *SIAM Jour. Math. Anal.* 15:723–736, 1984.
15. Haar, A. Zur Theorie der Orthogonalen Funktionensysteme. [in German] *Math Analysis* 69:331–371, 1910.
16. Healy Jr., D. M., and J. B. Weaver. Two applications of Wavelet Transform in magnetic resonance imaging. *IEEE Trans. Info. Theory.* 38:840–860, 1992.
17. Kadambe, S., and G. F. Bourdreaux-Bartels. Applications of the wavelet transform for pitch detection of speech signals. *IEEE Trans. Info. Theory.* 38:917–924, 1992.
18. Mallat, S. A theory for multiresolution signal decomposition: The wavelet representation. *IEEE Trans. Patt. Anal. Mach. Intel.* 11:674–693, 1989.
19. Mallat, S., and S. Zhong. Characterization of signals from multiscale edges. *IEEE Trans. Patt. Anal. Mach. Intel.* 14:710–732, 1992.
20. Mallat, S., and S. Zhong. Matching pursuits with time-frequency dictionaries. *IEEE Trans. Signal Processing.* 12:3397–3415, 1993.
21. Martinet, R. K., J. Morlet, and A. Grossman. Analysis of sound patterns through wavelet transforms. *Int. J. Patt. Recogn. Art. Intel.* 1:273–302, 1987.
22. Meste, O., H. Rix, R. Jau,and P. Cardinal. Detection of late potentials by means of Wavelet Transform. *Proc. IEEE Eng. Med. Biol. Soc.* 28–29, 1989.
23. Meyer, Y. *Wavelets, Algorithms and Applications*. SIAM, 1993.
24. Morlet, D., F. Peyrin, P . Desseigne, and P. Rubel. Wavelet analysis of high-resolution signal averaged ECGs in postinfarction patients. *J. Electrocardiology.* 26:311–320, 1993.
25. Rioul, O., and M. Vetterli. Wavelets and signal processing. *IEEE Signal Proc. Magazine,* 8:14–38, 1991.
26. Rioul, O., P. Duhamel. Fast algorithms for discrete and continuous wavelet transforms. *IEEE Trans. Info. Theory.* 38:569–586, 1992.
27. Schoenberg, I. J. Cardinal interpolation and spline functions. *J. Approx. Theory.* 2:167–206, 1969.
28. Shensa, M. J. Affine wavelets: Wedding the a trous and Mallat lags. *IEEE Trans. Signal Processing.* 40:2464–2482, 1992.
29. Tewfik, A. H., D. Sinha, and P. Jorgensen. On the optimal choice of a wavelet for signal representation. *IEEE Trans. Info. Theory.* 38:747–765, 1992.
30. Thakor, N. V., X. Gou, Y-C. Sun, and D. F. Hanley. Multiresolution wavelet analysis of evoked potentials. *IEEE Trans. BME.* 40:1085–1094, 1993.
31. Unser, M., A. Aldroubi, and M. Eden. On assimptotic convergence of B-spline wavelets to Gabor functions. *IEEE Trans. Info. Theory.* 38:864–872, 1992.
32. Vetterli, M., and C. Harley. Wavelets and filter banks: Relationships and new results. *Proceedings 1990 IEEE Int. Conf. Acoust., Speech, Signal Proc.* 1723–1726, 1990.
33. Vetterli, M., and C. Harley. Wavelets and filter banks: Theory and design. *IEEE Trans. Signal Proc.* 40:2207–2232, 1992.
34. Yang, X., K. Wang, and S. A. Shamma. Auditory representation of acoustic signals. *IEEE Trans. Info. Theory.* 38:824–839, 1992.

NOMENCLATURE

Note: all integral limits are from $-\infty$ to ∞ unless otherwise stated.

1. STFT = Short-Time Fourier Transform method
2. $\phi(t)$ = Scaling (basic dilation) functions
3. $\psi(t)$ = Wavelet functions
4. CWT = Continuous wavelet transform
5. * = Complex conjugation
6. a = Scaling factor
7. b = Time factor
8. R^+ = Real numbers
9. DWT = Discrete wavelet transform
10. $h(n)$ = Wavelet filter coefficients
11. $g(n)$ = Scaling filter coefficients
12. $A_{2^j}[x(n)] = a_{2^j}(k)$ = Scaling coefficients (approximate signal) at scale 2^j
13. $D_{2^j}[x(n)] = d_{2^j}(k)$ = Detailed signals (wavelet coefficients) at scale 2^j
14. $\psi_{2^j}(n - 2^jK)$ = Discrete wavelets at scale 2^j
15. $\phi_{2^j}(n - 2^jK)$ = Discrete scaling sequences at scale 2^j
16. Z = Set of integers
17. J = Numbers of maximum wavelet scales
18. FIR = Finite impulse response
19. QMF = Quadrature mirror filters